

Sorption of Fulvic Acids onto Titanium Dioxide Nanoparticles Extracted from Commercial Sunscreens: ToF-SIMS and High-Dimensional Data Analysis

Narjes Tayyebi Sabet Khomami ¹, Alexander Welle ^{2,3}, Stefan Kunz ¹ and Allan Philippe ^{1,*}

¹ Institute for Environmental Sciences (iES), Koblenz-Landau University, Fortstrasse 7, 76829 Landau, Germany; tayyebi@uni-landau.de (N.T.S.K.); stkunz@uni-landau.de (S.K.)

² Institute of Functional Interfaces, Karlsruhe Institute of Technology (KIT), 76344 Eggenstein-Leopoldshafen, Germany; alexander.welle@kit.edu

³ Karlsruhe Nano Micro Facility (KNMFi), Karlsruhe Institute of Technology (KIT), 76344 Eggenstein-Leopoldshafen, Germany

* Correspondence: philippe@uni-landau.de

Table S1. ID numbers, and SPF of the 10 studied sunscreens containing n-TiO₂. The detailed specification of each sunscreen can be found elsewhere [1].

Number	Trade Name ¹	Particle Shape [1]	Size (nm) ² [1]	Isoelectric Point [1]	Surface Coating ³ [1]	n-TiO ₂ content (mg) ⁴
1	Rewe Feuchtigkeits-Sonnenspray/ SPF (30)	Spherical, irregular	23.2 ± 1.2	2.6	PDMS	1.97 ± 0.14
2	Rewe Feuchtigkeits-Sonnencreme/ SPF (50)	Spherical and angular	28.0 ± 1.0	2.2	PDMS	2.23 ± 0.26
3	Real,-Quality Sonnenmilch/ SPF (30)	Ellipsoidal and angular	35.5 ± 2.0	1.7	PDMS	2.42 ± 0.18
4	Real,- Quality Sonnencreme/ SPF (30)	Spherical	19.3 ± 0.8	1.9	PDMS	1.66 ± 0.20
5	Biotherm Lait Solaire/ SPF (50)	Elongated	24.8 ± 0.8	1.9	PDMS	1.79 ± 0.09
6	Nivea Sun Pflegende Sonnenmilch/ SPF (50)	Spherical	34.3 ± 0.6	<1.8	SiO ₂	2.29 ± 0.35
7	Sundance Sonnenmilch/ SPF (50)	Ellipsoidal	30.8 ± 1.0	<1.8	PDMS	2.21 ± 0.33
8	Garnier Ambre Solaire Resisto Sonnenschutz-Milch/ SPF (50)	Elongated, spherical and ellipsoidal	22.3 ± 0.8	2.1	PDMS	2.63 ± 0.04
9	Alverde Sonnencreme Jojoba/ SPF (30)	Spherical, angular and elongated	35.6 ± 0.6	4.5	Al ₂ O ₃	3.38 ± 0.18
10	Baby sebamed Sonnenschutzlotion/ SPF (50)	Ellipsoidal and spherical	27.4 ± 1.7	3.1	Al ₂ O ₃ +SiO ₂	2.33 ± 0.18

¹ based on the information written on their packages.² average hydrodynamic diameter (nm)³ proposed surface coatings analyzed by ToF-SIMS.⁴ n-TiO₂ content extracted from 50 mg sunscreen (calculated based on the n-TiO₂ content in the initial sunscreen and the corresponding recoveries after the extraction [1]).

Table S2. Summary of random forest models performances.

	S3 ¹	S4 ²	S9 ³
Accuracy on test set (in %)	100	100	100
95% confidence interval in %	0.8456–1	0.8456–1	0.8456–1
mtry	85	50	2
Node size	1	1	1
Sample size	0.63	0.63	0.63
Out of bag error	0.04	0.00	0.00

¹n-TiO₂ ⊂ sunscreen (3) exposed to fulvic acids.²n-TiO₂ ⊂ sunscreen (4) exposed to fulvic acids.³n-TiO₂ ⊂ sunscreen (9) exposed to fulvic acids.

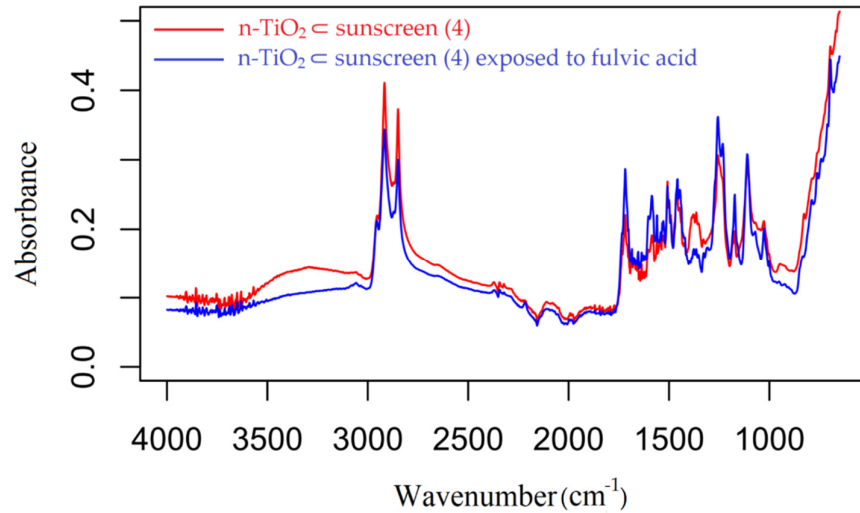


Figure S1. (a) Representative ATR-FTIR spectra of the n-TiO₂ ⊂ sunscreen (4) before and after exposure to fulvic acids. No presence of new bands or band shift is seen on the surface of n-TiO₂ ⊂ sunscreen (4) after exposure to fulvic acids (since the analysis was performed qualitatively, the changes in absorbance are not interpretable).

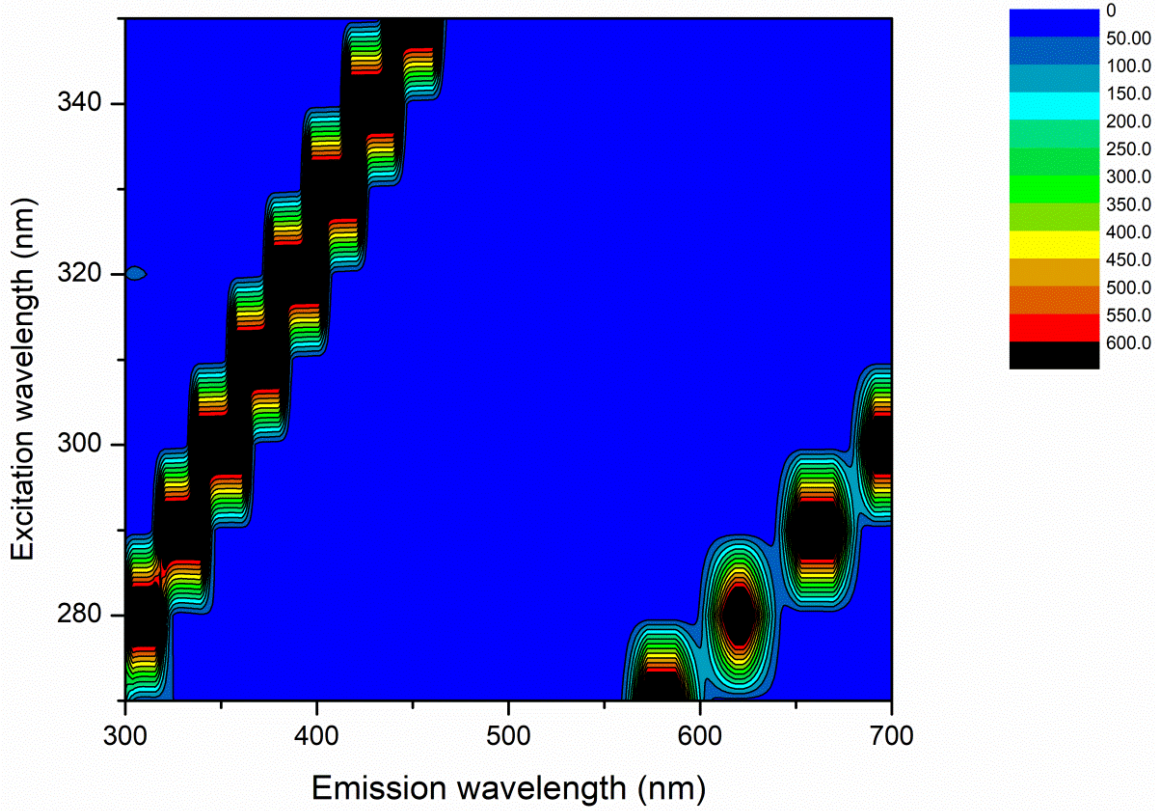


Figure S1. (b). Three-dimensional excitation-emission-matrix (EEM) fluorescence spectroscopy of n-TiO₂ ⊂ sunscreen(4) exposed to fulvic acid. No peaks depicting the presence of fulvic acids (excitation/emission ~ 310/450 nm) [2] can be detected on the nanoparticles (The color scale depicts the intensity, and the black lines depict fluorescence scattering).

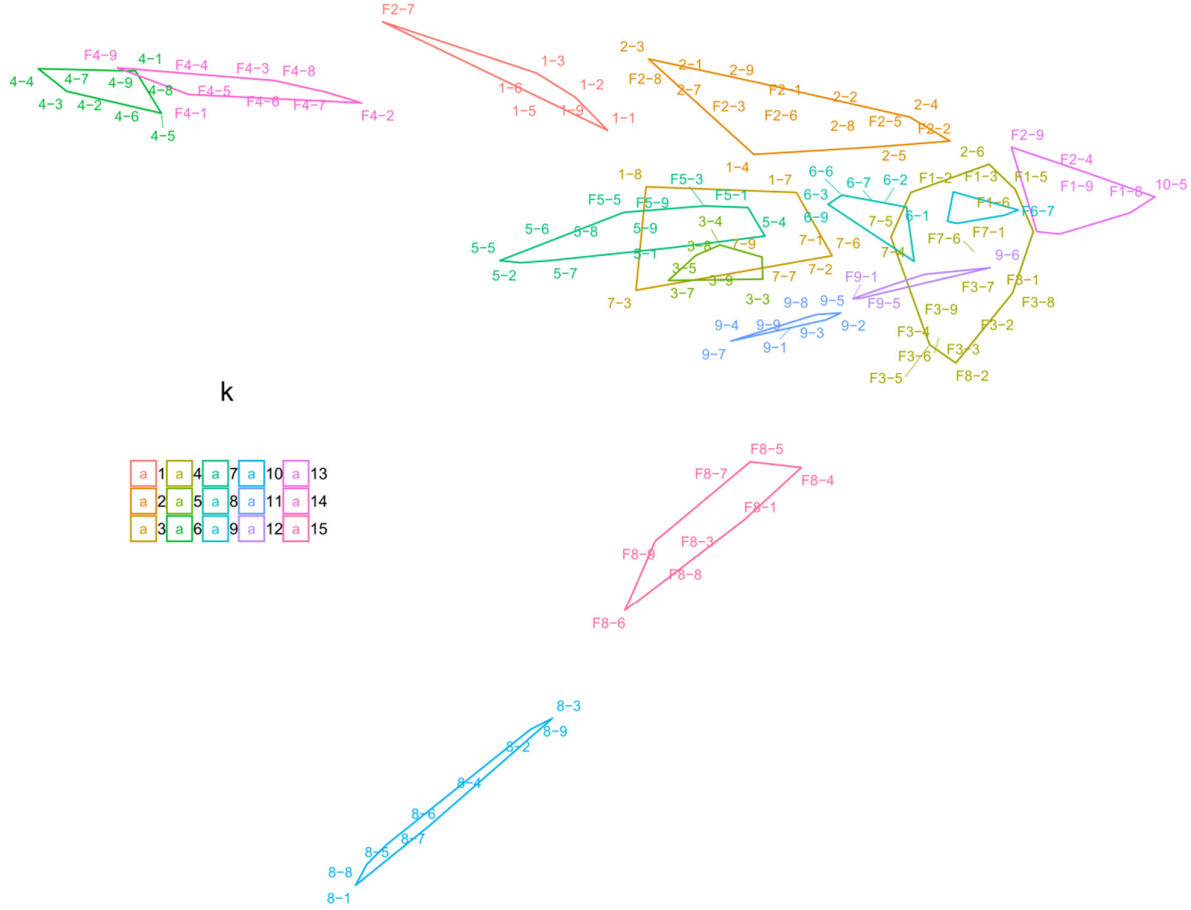


Figure S2. K-mean clustering of n-TiO₂ ⊂ sunscreen samples for 10 different sunscreens before (X-Y) and after (FX-Y) exposure to fulvic acid where X and Y depict the sunscreen's ID and the number of replicates, respectively. F represents the exposure to fulvic acids. K depicts the numbers of the clusters. Here, the optimized total number of clusters is 16. It has to be noted that the projection of the clusters on the 2D plane shown above is based on PCA, the overlapping of the clusters can be due to their projection in 2D. Since our data do not satisfy requirements for PCA (no linear gradient and skewed data), interpretation in terms of distances on the above graph should be avoided. Therefore, the projection on the plane formed by the two principal components is for visualization purposes only.

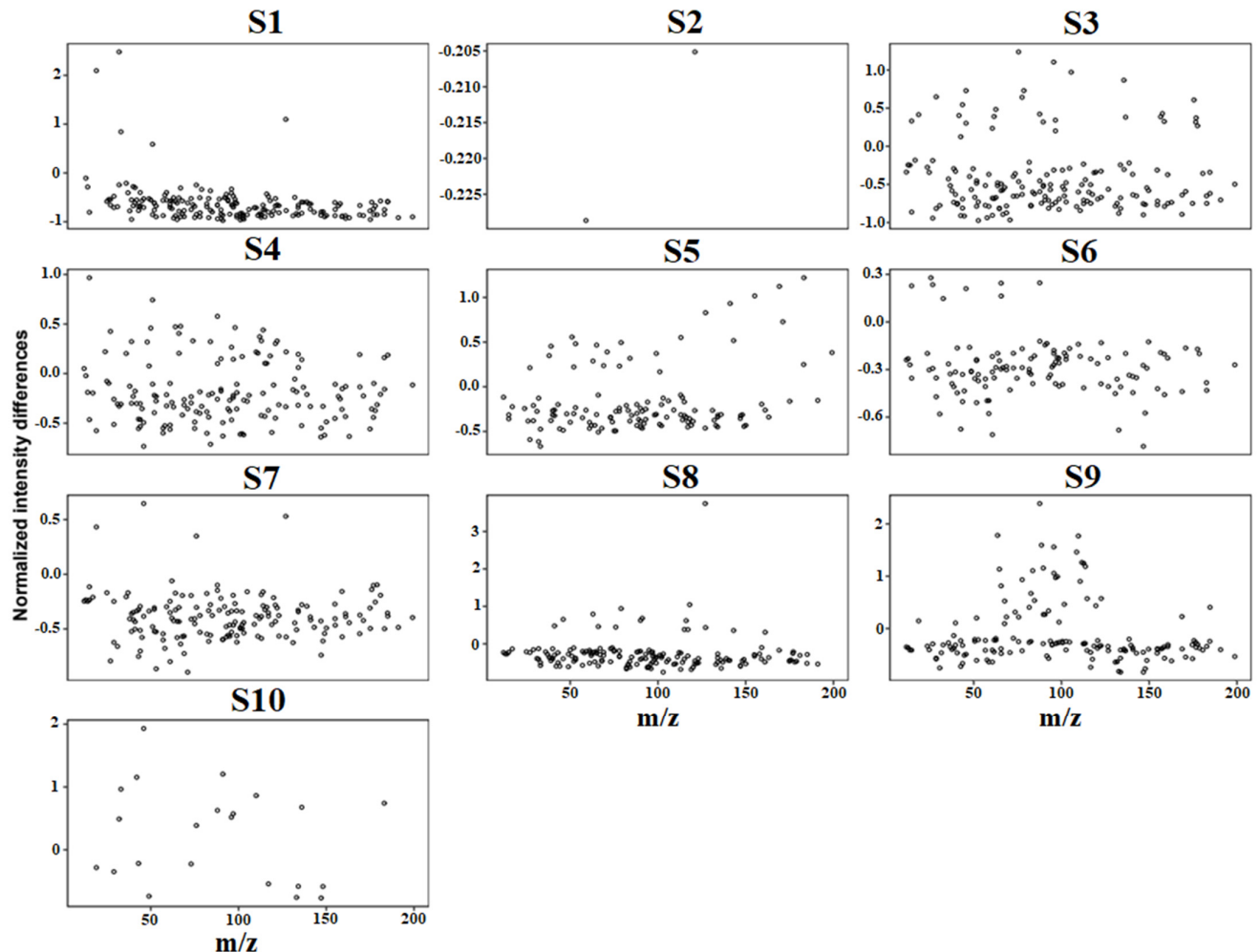


Figure S3. Significant (t-test 95% confidence) differences in the normalized intensities (negative polarity) averaged over 9 replicates for all masses detected using ToF-SIMS for n-TiO₂ in sunscreen samples before and after exposure to fulvic acids.

Table S3. The number of common masses^a of n-TiO₂ in sunscreen samples with increased-signal intensities after exposure to fulvic acids (X depicts the sunscreen's ID).

X	1	2	3	4	5	6	7	8	9	10
1	5									
2	0	0								
3	1	0	29							
4	1	0	1	40						
5	0	0	2	2	25					
6	1	0	2	5	0	8				
7	2	0	3	0	0	0	4			
8	1	0	4	5	4	1	3	16		
9	1	0	1	17 ^b	0	2	1	3	39	
10	1	0	5	4	1	2	2	3	2	12

^a Calculated from $F_X - X > 0$ i.e. differences of signal intensities of n-TiO₂ from the corresponding signal intensities of the same nanoparticles exposed to fulvic acids (9 replicates for each ToF-SIMS measurement). ^b The highest number of common masses (increased-intensity signals) is seen between samples 4 and 9 (17 common mass).

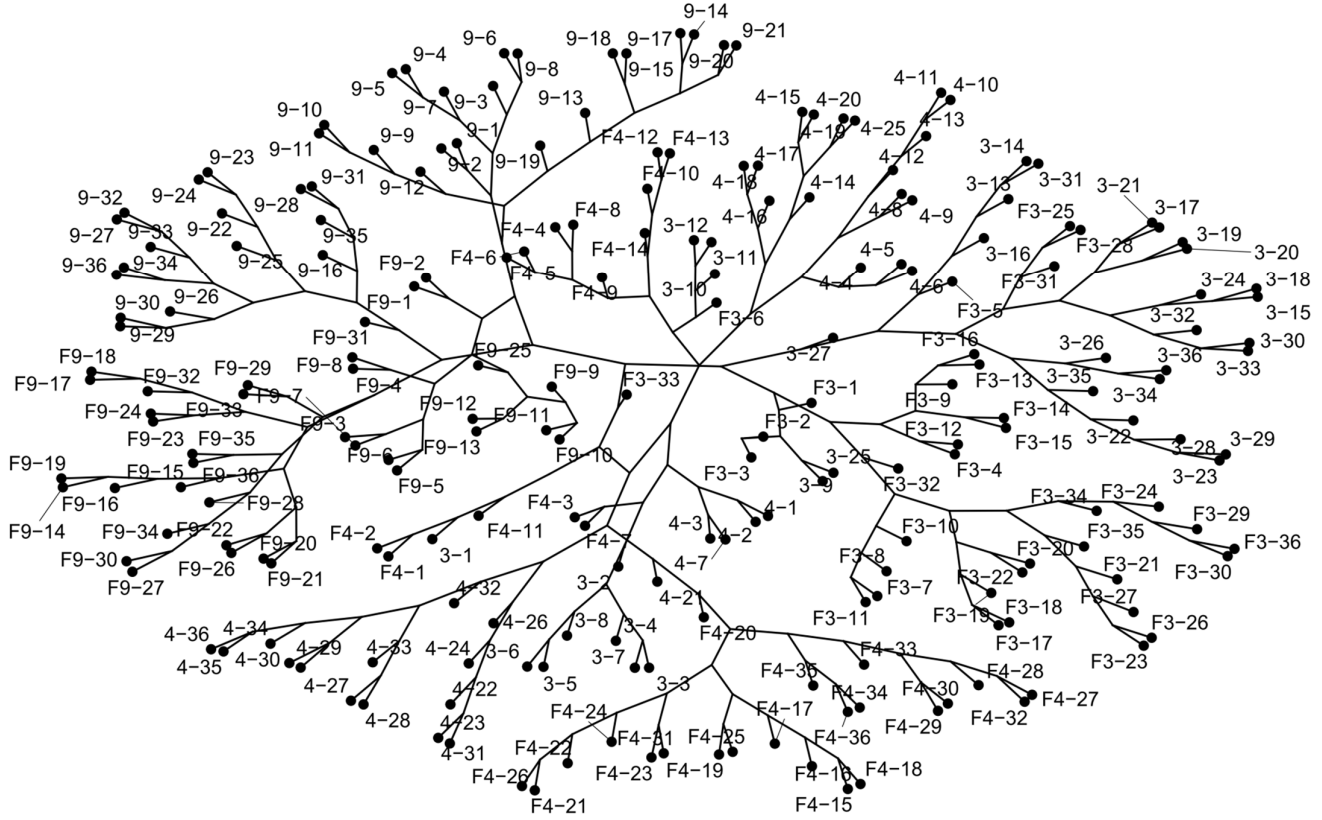


Figure S4. Visualization of the divisive hierarchical clustering of n-TiO₂-coated sunscreen samples (samples 3, 4, and 9) before (X-Y) and after (FX-Y) exposure to fulvic acids where X and Y depict the sunscreen's ID and the number of replicates, respectively. F represents the exposure to fulvic acids.

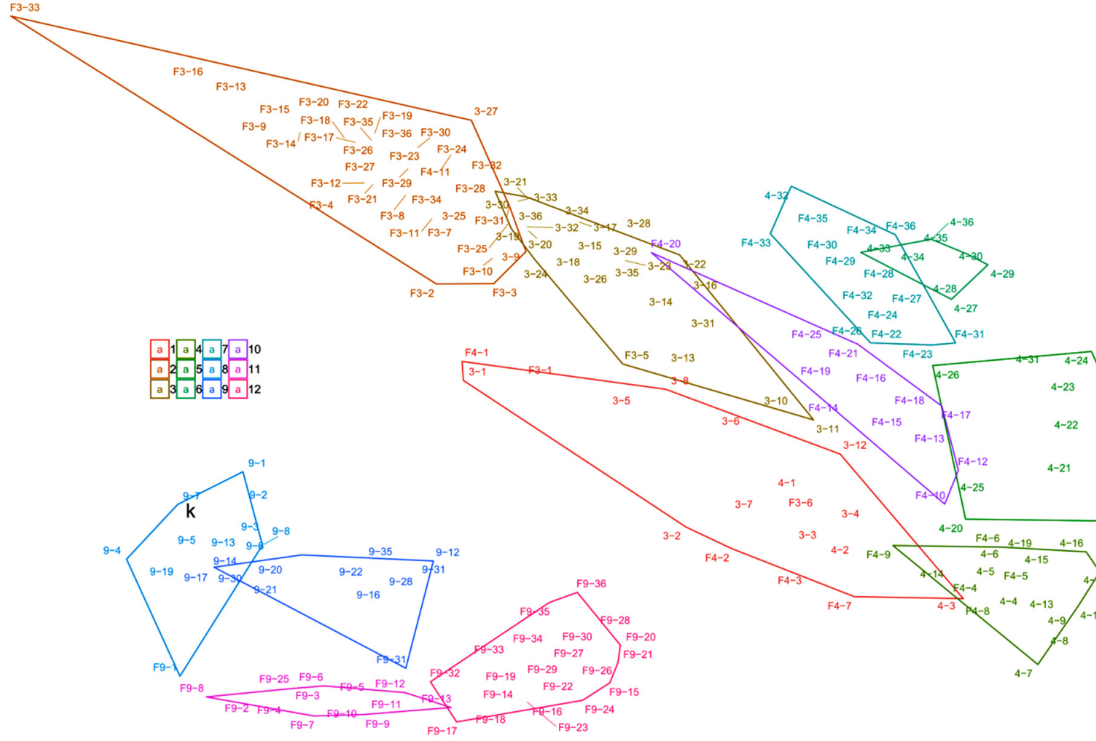


Figure S5. K-mean clustering of n-TiO₂ in sunscreens (samples 3, 4, and 9) before (X-Y) and after (FX-Y) exposure to fulvic acids where X and Y depict the sunscreen's ID and the number of replicates, respectively. F represents the samples exposed to fulvic acids. k depicts the optimized numbers of clusters. (Due to overlapping of the samples in 2D projection mode, not all the data points may be distinguishable).

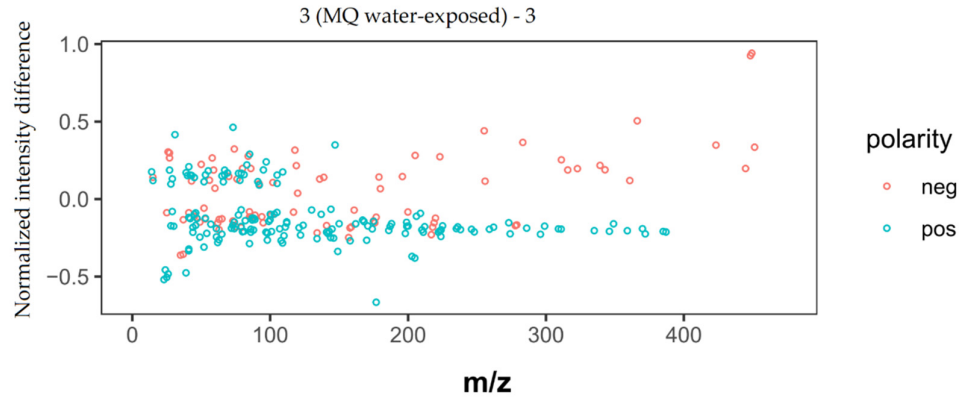


Figure S6. The intensity difference between 3 (MQ water-exposed)-3 where 3 (MQ water-exposed) is n-TiO₂ in sunscreen (3) exposed to pure water (instead of fulvic acids), and 3 depicts the initial n-TiO₂ in sunscreen (3). neg (red dots) depicts the negatively charged ions measured using ToF-SIMS, and pos (blue dots) depicts the positively charged ions measured using ToF-SIMS. MQ water is pure water.

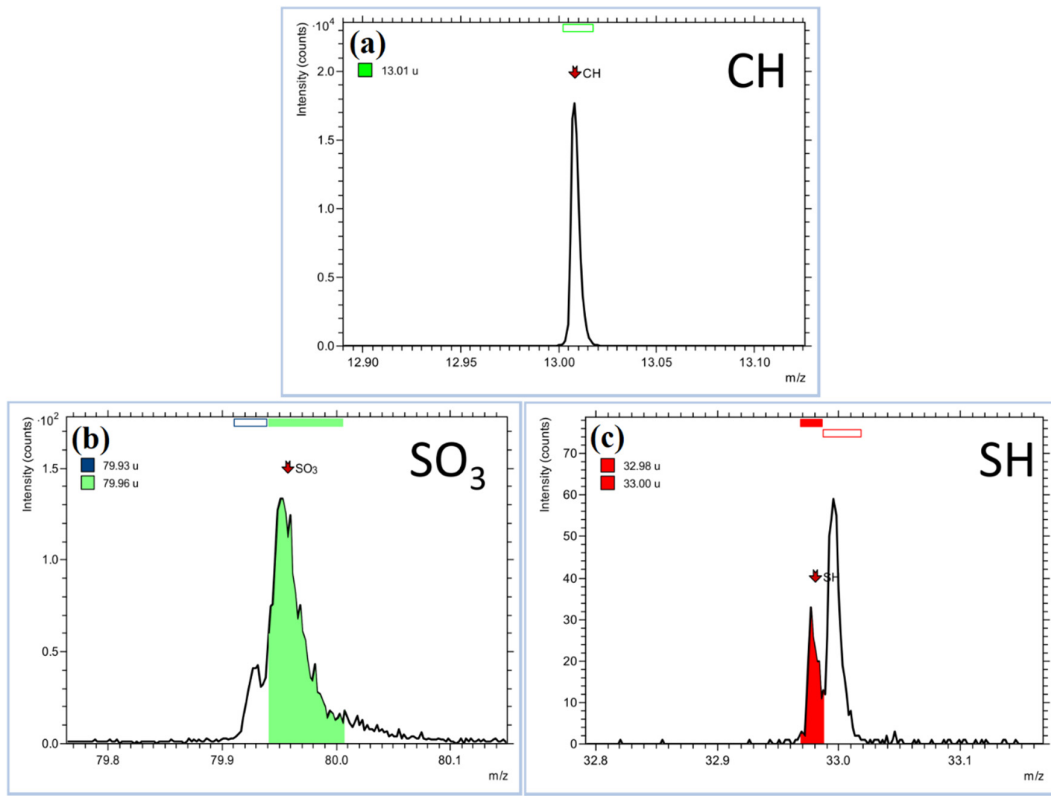


Figure S7. Mass (a) neg13.008 assigned to CH^- , (b) neg79.961 assigned SO_3^- and (c) neg32.98 assigned to SH^- on the surface of n-TiO₂⊂sunscreen (3) exposed to fulvic acids.

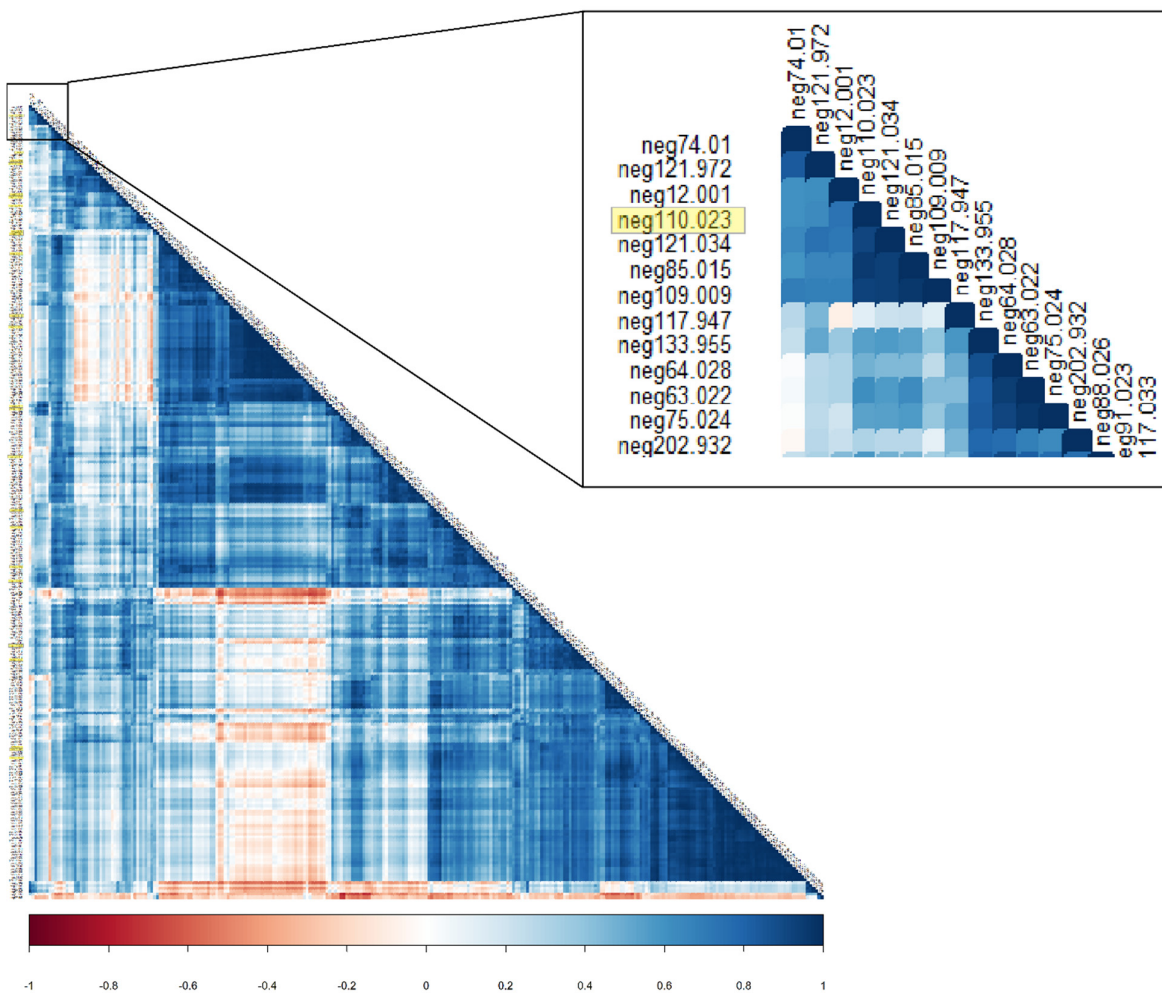


Figure S8. The correlation matrix of increased masses for sample F3 i.e. n-TiO₂ in sunscreen(3) exposed to fulvic acids. The variables are ordered using hierarchical clustering. Blue shows positive, and red shows negative correlations. The high-resolution image is available as a separate file on https://github.com/KunzstLD/Nanoparticle_classification.

References

- Philippe, A.; Kosik, J.; Welle, A.; Guigner, J.-M.; Clemens, O.; Schaumann, G. E. Extraction and characterization methods for titanium dioxide nanoparticles from commercialized sunscreens. *Environ. Sci. Nano* **2018**, *5*, 191–202.
- Yu, H.; Song, Y.; Liu, R.; Xi, B.; Du, E.; Xiao, S. Variation of dissolved fulvic acid from wetland measured by UV spectrum deconvolution and fluorescence excitation-emission matrix spectrum with self-organizing map. *J. Soils Sediments* **2014**, *14*, 1088–1097.